THE ASTROPHYSICAL JOURNAL, 475:740–753, 1997 February 1

THE THERMONUCLEAR EXPLOSION OF CHANDRASEKHAR MASS WHITE DWARFS

J. C. NIEMEYER AND S. E. WOOSLEY[1]
Max-Planck-Institut für Astrophysik, Karl-Schwarzschild-Strasse 1, 85740 Garching, Germany
Received 1995 October 4; accepted 1996 August 23

ABSTRACT

The flame born in the deep interior of a white dwarf that becomes a Type Ia supernova is subject to several instabilities, the combination of which determines the observational characteristics of the explosion. We briefly review these instabilities and discuss the length scales for which each dominates. Their cumulative effect is to accelerate the speed of the flame beyond its laminar value, but that acceleration has uncertain time and angle dependence which has allowed numerous solutions to be proposed (e.g., deflagration, delayed detonation, pulsational deflagration, and pulsational detonation). We discuss the conditions necessary for each of these events and the attendant uncertainties. A grid of critical masses for detonation in the range 10^7–2×10^9 g cm^{-3} is calculated and its sensitivity to composition explored. The conditions for prompt detonation are discussed. Such explosions are physically improbable and appear unlikely on observational grounds. Simple deflagrations require some means of boosting the flame speed beyond what currently exists in the literature. "Active turbulent combustion" and multipoint ignition are presented as two plausible ways of doing this. A deflagration that moves at the "Sharp-Wheeler" speed, $0.1 g_{\rm eff} t$, is calculated in one dimension and shows that a healthy explosion is possible in a simple deflagration if fuel can be efficiently burned behind a front that moves with the speed of the fastest floating bubbles generated by the nonlinear Rayleigh-Taylor instability. The relevance of the transition to the "distributed regime" of turbulent nuclear burning is discussed for delayed and pulsational detonations. This happens when the flame speed has slowed to the point that turbulence can actually penetrate the flame thickness and may be advantageous for producing the high fuel temperatures and gentle temperature gradients necessary for detonation. No model emerges without difficulties, but detonation in the distributed regime is plausible, will produce intermediate-mass elements, and warrants further study. The other two leading models, simple deflagration and pulsational detonation, are mutually exclusive.

Subject headings: hydrodynamics — instabilities — stars: interiors — supernovae: general — white dwarfs

1. INTRODUCTION

Despite 25 years of intensive investigation (e.g., Arnett 1969), the basic physics whereby a carbon-oxygen core of nearly the Chandrasekhar mass (1.39 $M_\odot$) explodes as a Type Ia supernova (SN Ia) is still debated. One may reasonably conclude that it is a hard problem. In fact, only recently has the astrophysics community begun to profit from the extensive experience of the chemical combustion community in order to appreciate fully just how complicated burning coupled to hydrodynamics really can be.

The astrophysical problem is especially hard because the nuclear flame propagates in an extensive medium in which gravity plays a role and several instabilities have time to develop over a large range of length scales. Any realistic solution must take cognizance of these instabilities and, if only by parameterization, incorporate them into the stellar model.

This need, and variability in the outcome depending on uncertain parameters, has given rise to several classes of supernova models, all largely empirical. These include the "delayed detonation" (Khokhlov 1991a, 1991b, 1991c; Woosley & Weaver 1994); "pulsational detonation" (Arnett & Livne 1994a, 1994b); "pulsational deflagration" (Nomoto, Sugimoto, & Neo 1976; Ivanova, Imshennik, & Chechetkin 1974); "convective deflagration" (Nomoto, Thielemann, & Yokoi 1984); and the fractal model of Woosley (1990), each of which, by various contrivances, generates a flame which is born slow and accelerates very rapidly as the star begins to come apart. This behavior has been found essential to obtaining nucleosynthesis that agrees with spectroscopic observations.

There are two simple solutions to the explosion problem, neither of which is thought to be correct, but which bound the real solution: (*a*) a laminar conductive flame and (*b*) prompt detonation. The latter is improbable (§ 3.2.2) and would give unacceptable nucleosynthesis (no intermediate-mass elements); the former is unphysical and would not give an energetic explosion. Between these two extremes lies the regime of unstable flame propagation, to which this paper is mostly devoted. We begin by reviewing the relevant instabilities and current views regarding their importance and mutual couplings. Although much has been written, especially regarding the Rayleigh-Taylor (RT) instability, not all share the same views even on this fundamental subject. It is therefore necessary to state (our view of) the basics before proceeding to the models, and so we briefly discuss (§ 2) the RT-instability, the Landau-Darrieus (LD) instability, the Kelvin-Helmholtz (KH) instability, and turbulence. Our main goals here are the following: (1) ascertaining the uncertainties in the models in an attempt to resolve the leading candidate(s); and (2) exploring the implications of new physics—active turbulent combustion, multipoint ignition, and, especially, detonation in the distributed regime—for models for SN Ia's.

[1] Permanent address: Board of Studies in Astronomy and Astrophysics, University of California, Santa Cruz, CA 95064.

It is frequently stated (Khokhlov 1995; Arnett & Livne 1994a) that simple deflagrations, those in which the flame remains at all times subsonic and in which an intervening pulse of the white dwarf does not occur, cannot give an energetic explosion. We discuss why this may not be true, either because of physics that has been left out of the calculations (§§ 3.1.2, 3.1.3) or because the flame has not been modeled sufficiently accurately in three dimensions (§ 3.1.1).

Another important point that has not been adequately discussed in the context of astrophysical flames, is the idea of "distributed burning." As long as the thickness of the flame is negligible, it can be treated as a temperature discontinuity. Heat never moves far from the burning surface. This is the case during most of the flame's life. But for densities below $\sim 3 \times 10^7$ g cm^{-3}, turbulence will disrupt the flame sheet. Once this happens, one can no longer speak of the flame as either laminar or conductive. It has entered a domain where turbulent transport directly affects the nuclear reaction region and smears it out over macroscopic length scales. The combustion community calls this type of burning the "distributed flame regime" (e.g., Pope 1987), and it is a frontier topic for them as well as us. While the increased mixing of hot ash and cold fuel can, in some instances, be beneficial for provoking a detonation, the same process also leads to compositional mixing, which increases the critical mass required for detonation to occur (§ 3.2.1). In § 3.2.5 we discuss the physical conditions required for this sort of detonation and show that it is a reasonable, if uncertain, occurrence. In this sense, it is superior to many other models in the literature.

Much has been written about other forms of the "delayed detonation model" (e.g., Khokhlov 1991a, 1991b, 1991c; Woosley & Weaver 1994), yet the physics of the transition to detonation remains obscure. In §§ 3.2.4 and 3.2.5 we discuss the two different kinds of delayed detonation that have been previously published and why each is unlikely to occur.

In the conclusions (§ 4) we summarize our results.

2. FLAME DYNAMICS AT HIGH DENSITIES

2.1. *The Conductive Laminar Flame*

The simplest solution to the propagation of burning in a premixed fuel is an elementary "flame." Heat is transported ahead of the burning region, in this case, by electron conduction. The temperature rises to the point where reactions can consume the fuel (carbon) on a diffusive timescale, and this condition sets both the thickness of the flame and its steady velocity (Landau & Lifshitz 1991). In the absence of instabilities, these quantities can be determined analytically with considerable precision (Timmes & Woosley 1992).

The critical mass required to keep a flame alive is small, a few times $(4/3)\pi\rho l_{\rm th}^3$, where $l_{\rm th}$ is the flame thickness. For isolated regions below this mass, heat can diffuse out and the flame will die, but so long as a critical mass remains intact, one cannot extract heat from the ashes of the combustion (in order to raise the temperature of the fuel) over a greater distance than $l_{\rm th}$. It is impossible for a simple *laminar* flame to turn into a detonation. As long as there is a flame with a well-defined surface (exceptions to this will be discussed in §§ 2.6 and 3.2.5), detonation can only be achieved by increasing the area of the flame.

It is well known that the laminar speed is too slow to make a supernova with the observed properties. In fact, we shall conclude (see also Niemeyer & Hillebrandt 1995b and Khokhlov 1995) that the laminar speed is not very relevant for the effective rate at which burning spreads. Turbulence and RT instabilities are more important and carry the flame at a speed independent of the microphysics. However, it is important to keep track of the flame *thickness*, since this may ultimately affect even the macroscopic nature of the burning, and to distinguish the speed with which the outer boundary of burning spreads from the total rate of mass consumption. These rates are quite different if a large amount of fuel becomes entrained.

After a brief review of the various instabilities that arise from a linear analysis of flame propagation under the influence of gravity and shear in § 2.2, we discuss the quasi-stationary structure of the flame surface after it reaches the fully nonlinear regime in §§ 2.3, 2.4, and 2.5.

2.2. *Linear Instabilities*

The problem of linear hydrodynamical stability of subsonic flames in the thin-flame representation was first analyzed by Darrieus (1938) and, independently, by Landau (1944). Landau's result for the linear growth rate also includes the influence of gravity on the density jump produced by the flame front, which is equivalent to the RT instability (Chandrasekhar 1961) if the flame speed is set to zero. In the context of nuclear flames in degenerate carbon, the LD instability has been explored in detail both analytically and numerically by Blinnikov & Sasorov (1996) and Bychkov & Liberman (1995), and its onset has been demonstrated by means of two-dimensional hydrodynamical simulations (Niemeyer & Hillebrandt 1995a). All these studies agree that on scales larger than the Markstein, or critical, length $l_{\rm crit} \approx 100 l_{\rm th}$ (Markstein 1951), flames moving upward are unstable to both LD and RT instabilities on all wavelengths.

In addition to radial perturbations, we have to consider perturbations that face in a direction perpendicular to gravity, where buoyancy of burned material floating in the cold fuel induces tangential velocity differences along the flame surface. Here, another instability becomes important, the KH or shear instability (e.g., Landau & Lifshitz 1991). In our context, it is quite important to know the circumstances under which the flame surface in a Type Ia supernova is KH-unstable, since this condition marks the transition to the fully turbulent burning regime. Strictly speaking, tangential discontinuities can only occur if the mass flux through the surface vanishes, for otherwise continuity of the momentum flux imposes continuity of the tangential velocity components. The mass flux through the burning zone is by definition nonzero. Thus, we can qualitatively argue that the propagation of a flame tends to stabilize the front against KH instability. If, however, the flow field around a burning bubble is dominated by buoyant acceleration, i.e., the mass flux becomes small compared with the velocity components tangential to the front, the flame becomes KH-unstable, as shown by numerical simulations (Niemeyer & Hillebrandt 1996). This occurs during the nonlinear stage of the RT instability.

2.3. *The Cellular Regime*

In the nonlinear evolution of the LD instability, the formation of cusps at the points where the flame front self-intersects gives rise to an additional quadratic damping term for the perturbation amplitude that is not included in

Landau's linear stability analysis (Zeldovich et al. 1985). It stabilizes the flame surface after cells with a stationary, scale-independent amplitude have formed. The speed of the emerging cellular surface is directly given by the increased surface area, yielding

$$u_{\rm cell} = u_{\rm lam}[1 + \epsilon(\mu)] \ , \tag{1}$$

where the velocity increment ϵ is a function of the gas expansion parameter $\mu = \rho_{\rm b}/\rho_{\rm u}$ (Zeldovich 1966). If μ is small, as in the case of burning in degenerate matter, ϵ can be approximated by (Zeldovich 1966)

$$\epsilon(\mu) = \frac{\pi^2}{24}(1-\mu)^2 \approx 0.41(1-\mu)^2 \ . \tag{2}$$

Motivated by the large dynamical range of thermonuclear flames in white dwarfs, Blinnikov & Sasorov (1996) proposed a fractal model for the cellular structure of LD unstable flames. By means of a statistical analysis of the Sivashinsky equation for thin-flame propagation, the authors estimated the fractal dimension of one-dimensional flames as

$$D_{1d} = 1 + D_0 \gamma^2 \ , \tag{3}$$

where $\gamma = (1 - \mu)$. This result was confirmed by numerical simulations of the closely related Frankel equation, which yielded $D_0 \approx 0.3$. Furthermore, the authors derived the fractal dimension of two-dimensional flame surfaces as $D_{2d} \approx 2D_{1d}$.

Here we take a simplified approach that shows how D_0 of one-dimensional cellular flame fronts can be related to ϵ. By doing so, we neglect some subtle, but important, complications that arise in the statistical treatment of the Sivashinsky equation which are accounted for in the more sophisticated approach of Blinnikov & Sasorov (1996). In our simple model, we describe the cellular front as a hierarchy of cells on all length scales. If consecutive cell generations are widely separated, we can assume that the thin-flame approximation is valid on each scale. The effective propagation speed u_i on scale l_i is then related to scale $l_{i-1} < l_i$ by

$$u_i = u_{i-1} + \epsilon u_{i-1} \ . \tag{4}$$

Taking the continuum limit and integrating yields

$$u_i = u_0 \, e^{\epsilon i} \ . \tag{5}$$

We now assume that cell splitting occurs after a dilation interval S, so that $l_i = S l_{i-1}$. If the smallest unstable length scale is of the order of the Markstein length, $l_0 = l_{\rm crit}$, we find $l_i = S^i l_{\rm crit}$, and we can express the effective flame velocity in terms of the length scale l:

$$u_{\rm cell}(l) \approx u_{\rm lam}\left(\frac{l}{l_{\rm crit}}\right)^{\epsilon/\ln S} \ . \tag{6}$$

If the flame speed is interpreted in a geometrical way, i.e., $u(l) \propto \bar{A}_l$, where $\bar{A}_l$ denotes the increased surface of a cellular front observed at the scale l, it follows that the surface area behaves like a fractal (Mandelbrot 1983):

$$\bar{A}_l = A_{\rm lam}\left(\frac{l}{l_{\rm crit}}\right)^{D_{\rm cell}-1} \ , \tag{7}$$

with the fractal dimension

$$D_{\rm cell} = 1 + \frac{\epsilon}{\ln S} \ . \tag{8}$$

Inserting equation (2) in equation (8), we find, in agreement with Blinnikov & Sasorov (1996), that the fractal excess of equation (8) is proportional to $\gamma^2 = (1 - \mu)^2$. Specifically, we find $D_0 = \pi^2/24 \ln S$, and agreement with the authors' numerical results yields a dilation interval, $S \approx 4$.

2.4. *Nuclear Burning in the Flamelet Regime*

In the case of a cellular flame front driven purely by the LD instability, i.e. in the absence of gravity, there is no known upper limit for the largest scale of cell formation. However, if gravity is turned on, the cell structure is no longer scale independent, which leads to the breakdown of nonlinear stabilization (Khokhlov 1995). As soon as the process of cell disruption and bubble formation occurs on the largest scales, a cascade of turbulent velocity fluctuations is produced that continues on scales below the actual large-scale flame instability (Niemeyer & Hillebrandt 1995b). After the establishment of the turbulent cascade, there exists a range of scales where burning is dominated by isotropic, fully developed turbulence. We will restrict our discussion to the conservative assumption that the production of turbulence is provided purely by large-scale fluid instabilities, so that turbulent burning can be called "passive." Some thoughts on "active" turbulent combustion, where thermal expansion within the burning region is assumed to influence the properties of turbulence, are given in § 3.1.2.

Cell formation ceases on the scale l where the turbulent velocity fluctuations $v(l)$ become comparable to $u_{\rm cell}(l)$. Here the time of front interaction with turbulent eddies becomes comparable to the eddy turnover time and, consequently, perturbations caused by turbulence grow to amplitudes comparable to the cell amplitudes. The cellular flame front is thus unstable on these scales (Zeldovich et al. 1980). Furthermore, numerical simulations of curved flames subject to shear show the breakdown of the nonlinear stabilization mechanism if $v_{\rm shear} \approx u_{\rm cell}$ (Niemeyer & Hillebrandt 1996). The transition between cellular and turbulent burning regimes is therefore marked by the Gibson scale, defined as (Peters 1988)

$$v(l_{\rm Gibs}) = u_{\rm cell}(l_{\rm Gibs}) \ . \tag{9}$$

Note that, on the basis of the arguments above, we take equation (9) as an equality, which differs from earlier results (Khokhlov 1995) where the smallest turbulent scale was found to be $\approx 500 l_{\rm Gibs}$. Using the Kolmogorov scaling law $v(l) \propto l^{1/3}$, it follows that $l_{\rm Gibs}$ scales with the third power of $u_{\rm cell}/v(L)$, where $v(L)$ is, for instance, the magnitude of the turbulent velocity on the largest turbulent scale L. If we assume that near the beginning of the explosion this ratio is close to unity, implying that $l_{\rm Gibs} \approx L$, and later decreases owing to the decreasing flame speed and the buildup of shear in the RT mixing region, we find that the Gibson length decreases continually during the explosion. An upper bound for the intensity of turbulence on large scales is given by the "freezing out" of turbulent motions as a result of the overall expansion of the star (Khokhlov 1995). Using $v(L) \lesssim 10^7$ cm s^{-1} at $L \approx 10^6$ cm and $u_{\rm cell} \approx u_{\rm lam} \gtrsim 10^5$ cm s^{-1} (Timmes & Woosley 1992), we estimate that $l_{\rm Gibs} \gtrsim 1$

cm. Consequently, $l_{\rm Gibs} \gtrsim l_{\rm th}$ for all densities $\rho \gtrsim 3 \times 10^7$ g cm^{-3}. For this reason, turbulent nuclear flame fronts in white dwarf matter at these densities burn in the "corrugated flamelet regime" (e.g., Clavin 1994). At lower densities, the flame front enters the so-called distributed regime that will be described in §§ 2.6 and 3.2.5.

The flamelet regime is characterized by laminar flame propagation on microscopic scales, while burning is determined purely by turbulence on large scales and is therefore independent of microphysics. Fuel "digestion" occurs in an extended region behind the boundary of fuel and ashes, the so-called turbulent flame brush. The size of this region and the range of turbulent length scales adapt in a way that provides a flame-brush propagation velocity that is decoupled from the laminar flame speed. On scales obeying $l \gg l_{\rm Gibs}$, one can express the effective flame speed, $u_{\rm tur}(l)$, and turbulent front width, $d_{\rm tur}(l)$, in terms of l and the turbulent velocity $v(l)$ (Kerstein 1988; Clavin 1990), since both transport of burning fluid into the fresh material and fuel consumption inside the flame brush are limited by the eddy turnover time $\tau_t(l) \approx l/v(l) \propto l^{2/3}$. Consequently, the relations

$$u_{\rm tur}(l) \approx v(l) \ , \quad d_{\rm tur}(l) \approx l \tag{10}$$

are reasonable order-of-magnitude approximations that have been employed extensively in combustion research in the limit $v(l) \gg u_{\rm lam}$.

2.5. *The Rayleigh-Taylor Regime*

On the largest scales ($l \gtrsim 10^6$ cm) the flame dynamics is dominated by buoyancy of the hot, burned material surrounded by denser carbon and oxygen. The linearized problem is expressed by the RT instability (Chandrasekhar 1961). After a short period of exponential growth, the perturbation amplitudes become comparable to their wavelengths and the structure enters the nonlinear stage where interactions among the structures can occur, giving rise to merging and fragmentation of bubbles. Another important process is the appearance of KH-unstable regions along the bubble surfaces. These produce turbulent eddies that spread out bubble tips and walls. Finally, the long time evolution shows continuing merging and fragmentation of rising bubbles, creating an increasingly turbulent mixing layer (Snider & Andrews 1994).

Experiments of gas bubbles rising in vertical tubes filled with fluid were performed to measure the asymptotic velocity of a single bubble (Davies & Taylor 1949). Best fits to the measurements were obtained by the relation

$$v_{\rm RT} = \mathscr{B}\sqrt{g_{\rm eff}\, l} \ , \tag{11}$$

where $\mathscr{B} \in [0.466, 0.490]$ is a constant, $g_{\rm eff} = {\rm At}\ g$ is the effective gravitational acceleration [$ {\rm At} = (\rho_{\rm u} - \rho_{\rm b})/(\rho_{\rm u} + \rho_{\rm b}) \approx 0.5(1 - \mu)$ is the Atwood number], and l is the radius of the tube. Layzer (1955) solved the problem analytically for a spherically symmetric tube and derived $\mathscr{B} = 0.511$. Khokhlov (1995) derived a similar prescription for the propagation speed of RT-unstable flames in open boxes from numerical simulations. While this result is true for a single length scale, we need to consider a range of RT-unstable scales, where the front creates a large number of bubbles with various radii. The so-called Sharp-Wheeler model statistically describes the nonlinear stage of a multiscale RT front (Sharp 1984). It consists of a one-dimensional string of bubbles that are described by their radius, r_i, and height, z_i. According to equation (11), the heights grow as $\dot{z}_i = v_{\rm RT}$. Neighboring bubbles merge if the difference between their heights exceeds the radius of the smaller bubble and thus the average bubble radius increases with time. Consequently, the average rise velocity from equation (11) also grows. Numerical simulations of the Sharp-Wheeler model (Glimm & Li 1988) show that the front asymptotically attains a constant acceleration that is proportional to $g_{\rm eff}$, so that the RT mixing region grows at a rate of approximately

$$r_{\rm SW} \approx 0.05 g_{\rm eff}\, t^2 \ . \tag{12}$$

This result is in agreement with full hydrodynamical simulations (Young 1984) and experiments (Read 1984). Equivalently, we can say that the front advances into the cold material with a speed of

$$v_{\rm SW} \approx 0.1 g_{\rm eff}\, t \ . \tag{13}$$

Comparing equations (11), (12), and (13) shows that the maximum bubble radius evolves linearly with its displacement from the stellar center (i.e., the inner boundary of the RT mixing zone), $l_{\rm max} \propto r$.

In the context of supernova modeling, we are mainly interested in the burning velocity of the RT-unstable flame brush. As in § 2.4, we can argue that the overall burning rate is limited by the *fastest* transport mechanism that mixes ashes and fuel. Invoking the arguments of the previous section, fuel consumption automatically adjusts to the speed of fuel contamination by burning blobs in order to provide a burning rate that is independent of microphysics. The highest speed for each single length scale l is now given by equation (11), yielding $u_{\rm RT} \propto l^{1/2}$. A geometrical interpretation (eq. [7]) of the flame speed in the nonlinear RT regime therefore yields a fractal dimension of the flame surface, $D_{\rm RT} = 2.5$. In addition, we need the evolution of the maximum bubble size, $l_{\rm max}$, as a function of time or radial displacement, like the one provided by the Sharp-Wheeler model. If we assume that bubble growth is purely governed by merging, and that burning is completed somewhere within the RT mixing region (this need not necessarily be the case), the effective burning velocity is given by the Sharp-Wheeler speed (eq. [13]). One-dimensional supernova models using equation (13) will be presented in § 3.1.1.

Finally, we define the boundary between the turbulent burning regime dominated by Kolmogorov scaling and the buoyancy-driven RT regime by looking at the minimum timescale for self-interaction of flame structures with the size l, roughly given by $\tau_{\rm si}(l) \approx l/v_{\rm RT}(l) \propto l^{1/2}$. As stated above, expansion of the star inhibits the growth of the largest structures into the fully nonlinear regime where they become isotropically turbulent. Expansion is characterized by the hydrodynamical timescale $\tau_{\rm dyn} \approx 0.1$ s, so that self-interaction resulting in fully developed turbulence occurs on scales below $l_{\rm tur/RT}$ defined by $\tau_{\rm si}(l_{\rm tur/RT}) = \tau_{\rm dyn}$. Inserting equation (11) yields

$$l_{\rm tur/RT} = \tau_{\rm dyn}^2 \mathscr{B}^2 g_{\rm eff} \approx 10^6 \text{ cm} \ , \tag{14}$$

where we have used $g_{\rm eff} \approx 5 \times 10^8$ cm s^{-2} as a typical value for the effective gravitational acceleration.

2.6. *Summary of Instabilities and Their Effects*

Beginning at the smallest dynamically relevant scale, the thermal flame thickness, $l_{\rm th}$, the flame propagates with the laminar flame speed, $u_{\rm lam}$, until the smallest cells appear at

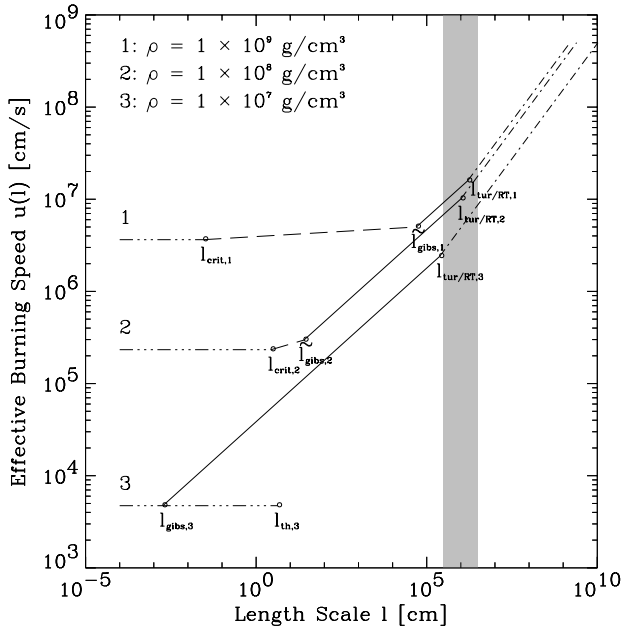

FIG. 1.—Effective burning speed as a function of length scale for the early, main, and late phases of the deflagration. The shaded region represents the typical resolution of multidimensional simulations, $\Delta \approx 10$ km.

$l_{\rm crit} \approx 100 l_{\rm th}$. Therefore, $u(l) = \text{const}\ (l)$. In the cellular regime, $u(l) \propto l^{D_{\rm cell}-2} \approx l^{0.1}$. Cellular stabilization fails when turbulent velocities become comparable to the effective cellular flame speed at $l_{\rm Gibs}$. As a result of the Kolmogorov scaling law for turbulent velocity fluctuations and the assumption that the turbulent flame speed is determined by the eddy turnover time on every scale, we find that $u(l) \propto l^{1/3}$ in the fully turbulent regime. Above $l_{\rm tur/RT}$, the largest upward velocity on scale l is determined by buoyancy. Hence, $u(l) \propto l^{1/2}$ according to equation (11). Figure 1 is a summary of the scale dependence of the burning speed $u(l)$. The piecewise scale-invariant burning regimes are represented by straight lines with different slopes in the log-log plot. Three separate curves are shown, corresponding to the characteristic velocities and length scales at early, central, and late times of the deflagration phase (as represented by three decreasing density values). All graphs are based on the assumption that all the relevant instabilities and the transitions between them have reached a statistical equilibrium state. This is true after approximately one growth time of the largest considered scale ($\approx$0.2 s).

The curves in Figure 1 are constructed as follows: First, the largest fully turbulent length scale $l_{\rm tur/RT}$ is computed from equation (14) with values for g taken from Khokhlov (1993a), while the burning speed at this scale is determined from equation (11). This point in the u-l plane serves as the origin for the purely buoyant part with $u(l) \propto l^{1/2}$ extending to larger l, and for the Kolmogorov part reaching downward. The laminar flame speed is used as the second absolute point of each graph. Its value, as well as the thermal flame thickness, $l_{\rm th}$, and the expansion factor, $\gamma = \Delta\rho/\rho$, are taken from Timmes & Woosley (1992). At a length of $l_{\rm crit} \approx 100 l_{\rm th}$, the LD instability and the subsequent formation of cells mark the transition to the scaling $u(l) \propto l^{D_{\rm cell}-2}$ with $D_{\rm cell} \approx 2(1 + 0.3\gamma^2)$ (Blinnikov & Sasorov 1996; § 2.3). This line is extended until it intersects the Kolmogorov line coming from above, which defines the Gibson scale $l_{\rm Gibs}$. Notice that, by virtue of this construction procedure reflecting our current understanding of flame dynamics in scale space, all burning properties above $l_{\rm Gibs}$ are uniquely fixed by large-scale phenomena and are therefore independent of microphysics.

The early phase of the explosion, where $\rho \approx 10^9$ g cm^{-3}, is characterized by a high laminar flame speed and small thermal expansion, resulting in a very shallow slope of $u(l)$ in the cellular regime. On scales of approximately 10 km, however, both effects are already dominated by the RT instability and turbulent burning. The turbulent regime becomes more pronounced as $u_{\rm lam}$ declines and the Gibson scale decreases ($\rho \approx 10^8$ g cm^{-3} [*second graph*]). Meanwhile, the cellular part of $u(l)$ becomes steeper owing to the increasing thermal expansion γ. In the simplified construction method outlined above, the highest turbulent velocities are assumed to be coupled directly to the RT velocity at the transition length $l_{\rm tur/RT}$. Consequently, the model implied here "forgets" about all turbulence that has been built up by earlier RT fluctuations, in contrast to the more realistic expectation that the level of turbulence decreases according to the almost negligible microscopic dissipation into heat. This assumption of instantaneous adjustment results in decreasing RT and turbulent flame speeds as the density—and therefore $g_{\rm eff}$ in equation (14)—falls. A phenomenological approach to account for the memory effect of accumulated turbulence in numerical simulations of SN Ia's has been proposed by Niemeyer & Hillebrandt (1995b).

Figure 1 also shows that our argument breaks down at the lowest density ($\rho \approx 10^7$ g cm^{-3}), represented in the bottom graph. Here the Gibson length, $l_{\rm Gibs}$, is smaller than the thermal flame thickness, $l_{\rm th}$, by almost 4 orders of magnitude. Therefore, the conditions for the flamelet regime (§ 2.4) are no longer satisfied, implying that laminar flame propagation ceases to occur on all scales (strictly speaking, this also implies that $l_{\rm Gibs}$ is no longer a well-defined quantity). Instead, turbulent eddies disrupt the burning

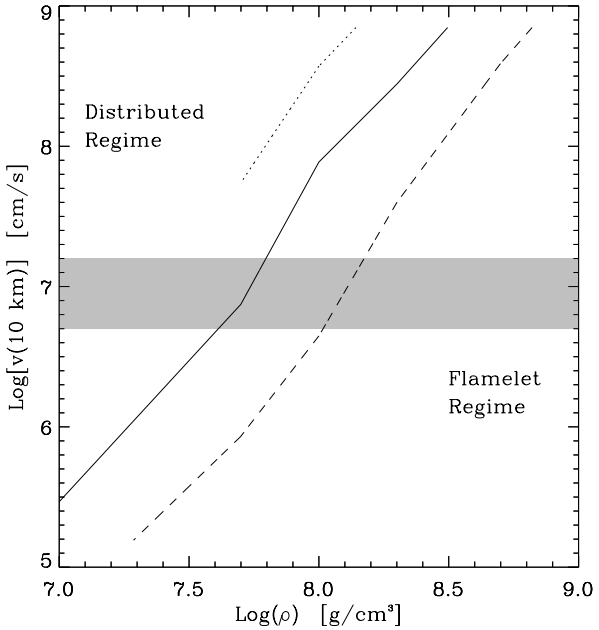

FIG. 2.—Regions of flamelet and distributed burning depending on fuel density and turbulent velocities at $L \approx 10$ km. The lines depict $l_{\rm th} = l_{\rm Gibs}$ for different compositions (*dashed line*: $X_{\rm C} = 0.2$; *dotted line*: $X_{\rm C} = 1$; *solid line*: $X_{\rm C} = 0.5$). The shaded region shows the range of turbulent fluctuations induced by the RT instability on large scales.

region and dominate over conductive transport even on microscopic scales. This burning regime is sometimes termed "distributed" or "stirred combustion" (e.g., Pope 1987). We emphasize that all of the preceding discussion is based sensitively upon the assumption of microscopic flamelets and therefore becomes largely invalid after the transition to the distributed burning regime. Regions of distributed and flamelet regimes are displayed in Figure 2 as a function of fuel density and macroscopic turbulent velocity v(10 km). The lines depict the transition defined by $l_{\rm th} = l_{\rm Gibs}$ for three different compositions. Decreasing carbon mass fraction is related to an earlier transition to distributed burning, since the flame thickness grows while the flame speed decreases.

3. HOW THE WHITE DWARF EXPLODES

3.1. *Deflagration*

3.1.1. *A Simple Deflagration?*

The simplest outcome to the exploding white dwarf problem would be a supernova in which the flame remained at all times and places subsonic and burned a sufficient fraction of the stellar mass to explode the star violently on the first attempt with no intervening pulsation. This is the basis for the common "deflagration" or "convective deflagration" model, of which W7 (Nomoto et al. 1984) is a popular example. Numerous studies of this model (and others like it, e.g., Woosley, Axelrod, & Weaver 1984; Woosley & Weaver 1994) give at least moderately good agreement with the observed light curve, spectrum, and nucleosynthetic requirements of common Type Ia events. The model does so by virtue of having approximately the correct proportions of intermediate-mass elements (Si–Ca) to ^{56}Ni and the right final ^{56}Ni mass for a Chandrasekhar mass starting point. This result is, in turn, a consequence of a flame speed that has been crafted to yield the desired result by a particular choice of transport algorithm (mixing-length convection) and scale parameter (the mixing length as a function of time). Knowing approximately the desired result is useful, but can the flame speed in a real deflagration behave in the required way?

Recent multidimensional calculations differ in their conclusions regarding this important issue. Khokhlov (1995) and Arnett & Livne (1994a) find that the flame moves too slowly to explode the star on the first try. Niemeyer & Hillebrandt (1995b) and Niemeyer, Hillebrandt, & Woosley (1996) find that a prompt explosion is possible, albeit a weak one that makes little ^{56}Ni. A key difference in these calculations is the treatment of turbulence. All assume that the RT instability is chiefly responsible for the production of turbulence, but while the former models assume that RT structures are isotropic and therefore implicitly employ an instantaneous adjustment of the turbulent cascade to the RT fluctuations, the latter simulations allow for a time delay between the production and dissipation of turbulent kinetic energy. They therefore include a "memory" for the history of the turbulent energy of each fluid element, which, in some cases, gives rise to a buildup of turbulence above its local equilibrium.

In the next sections, two physical ways of boosting the deflagration efficiency are discussed. A third possibility is simply that calculations having the necessary three-dimensional resolution and low numerical viscosity have yet to be done. Were it not for drag (admittedly an unreasonable omission), a buoyant bubble floating in response to its density contrast ($\sim$40% typically when the flame is at 1000 km) and local gravity ($\sim 10^{10}$ cm s^{-2}) would quickly achieve the sound speed. Assuming that the bubble dimension scaled linearly with distance from the center of the star, a reasonable assumption in the bubble cascade model of Sharp and Wheeler (Sharp 1984; § 2.5), specifically taking the bubble radius, $l_{\rm max} \sim 0.5r$, with r the distance to the stellar center and using equation (11), one obtains effective flame speeds $\sim$1500 km s^{-1}. This prescription implicitly includes drag, and the result is consistent with what is seen by Garcia-Senz & Woosley (1995) in analytic calculations and by Niemeyer et al. (1996) in two-dimensional numerical models. A similar result can be obtained by directly using the Sharp-Wheeler burning velocity (eq. [13]), which, for times 0.5–1 s, is again of order 1000–2000 km s^{-1}. Provided that turbulence is capable of burning out or "digesting" all material internal to the leading bubbles, this speed would be enough to generate at least a mild explosion (consistent with Niemeyer et al. 1996).

A simple one-dimensional calculation illustrating this possibility is given in Figure 3. A Chandrasekhar mass white dwarf was ignited at its center and given an effective flame speed that, after some time (0.5 s) during which the flame was assumed to move at a slow speed (approximately laminar), was assumed to be given by equation (13); $g_{\rm eff}$ was calculated each time step at the flame boundary. Calculations were done using the one-dimensional implicit hydrodynamics code KEPLER (Weaver, Zimmerman, & Woosley 1978), also described in § 3.2.1. This prescription assumes that the flame moves with a radial speed given for an ensemble of RT-unstable bubbles (Sharp 1984; § 2.5) and that turbulent processes behind the leading edge can "digest" all unburned fuel. The explosion is a healthy one, though short of intermediate-mass elements.

If for some reason the speed was greater, a stronger deflagration would result. Effects that have been left out of the simple Sharp-Wheeler speed (eq. [13]) are bubble growth by burning, which causes even small bubbles to merge, the negative heat capacity of a mixture of ^{56}Ni and α-particles (Garcia-Senz & Woosley 1995), and gradients in density and pressure.

3.1.2. *Active Turbulent Combustion?*

In § 2.4 we have neglected any feedback of burning itself on the intensity and spectrum of turbulence. In particular, we assume that the overall propagation speed of the turbulent flame brush is limited by the velocity of large-scale RT bubbles (eq. [11]). This need not be true. Owing to the limited range of observable scales, neither simulation nor experiment presently rules out the possibility that thermal expansion of burned material inside the flame brush significantly increases the strength of turbulent fluctuations on all turbulent scales. The energy available from nuclear burning is $\sim 10^{18}$ ergs g^{-1}, most of which goes into internal energy and bulk expansion of the star. Only a tiny fraction of this energy, $\sim 10^{14}$–10^{15} ergs g^{-1}, is injected into turbulence by the RT instability. Thus, the efficiency of any additional feedback mechanism that converts nuclear energy to turbulence need not be large. We therefore briefly discuss a possible mechanism for the feedback of burning on turbulence and its consequences for supernova explosions.

Thermal expansion behind the laminar flame is the main reason for the LD instability (§ 2.2). The growth of LD

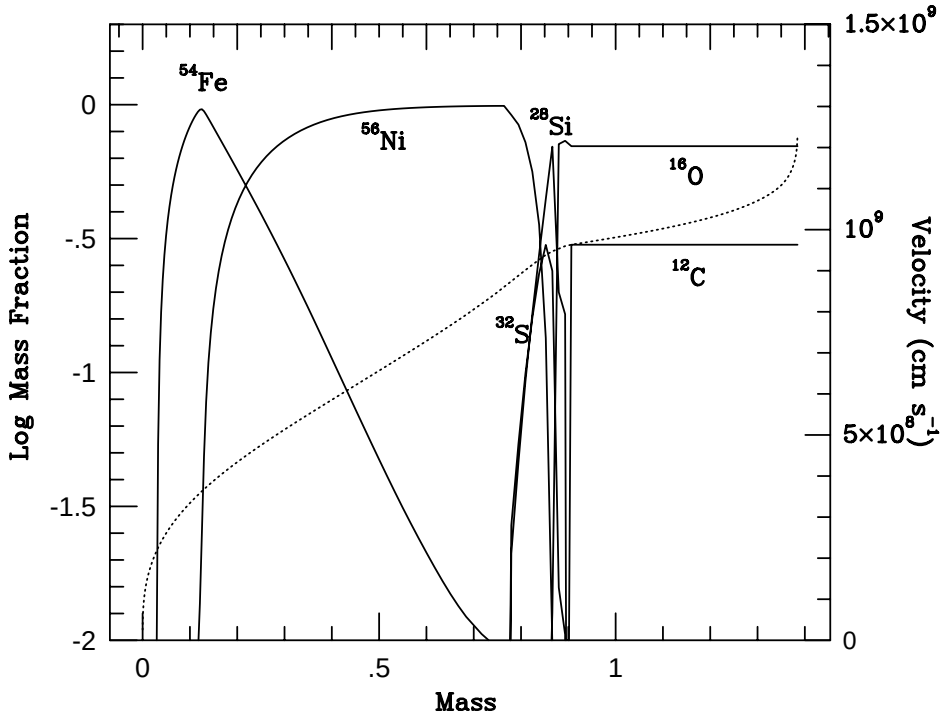

FIG. 3.—Final velocity and composition in a simple one-dimensional calculation of a deflagration in which the flame was constrained to move at a speed (in the comoving frame) of $0.1g_{\rm eff}(t - t_0)$ with $t_0 = 0.5$ s. The velocity is sampled at $t = 10$ s when it has taken on its coasting value. The final kinetic energy is 8.5×10^{50} ergs. The mass of ^{56}Ni is 0.57 $M_\odot$, and there are 0.24 $M_\odot$ of other iron group isotopes.

perturbations in the absence of external fluctuations is stopped by cusp formation leading to a stable cellular flame structure. It is possible, however, that once the cellular structure is disrupted by the turbulent cascade from above, the production of specific volume contributes again to the growth of velocity fluctuations. Although local intersections of flame segments resembling cellular cusps still occur in the turbulent regime, their random orientation inhibits the formation of any self-stabilizing structure. Instead, it is likely that neighboring expanding regions accelerate the medium in some stochastic direction, thereby enhancing the intensity of velocity fluctuations.

In a first approximation, we assume that this effect is most efficient on the scale of the expanding regions themselves and therefore does not significantly couple turbulent velocities on different scales. As a consequence, only the fluctuation amplitudes would be affected, not their spectrum. The simplest case would then be a constant and scale-independent growth rate, $\omega_{\rm tur}$, of turbulent velocity fluctuations on each scale that depended only upon the expansion parameter γ,

$$\frac{dv(l)}{dt} = \omega_{\rm tur}(\gamma)v(l) \, , \tag{15}$$

giving rise to exponential growth:

$$v(l, t) = v(l, 0)e^{\omega_{\rm tur}(\gamma)t} \, . \tag{16}$$

Since the most plausible functional dependence of $\omega_{\rm tur}$ on γ would be monotonically growing, this effect could readily account for the required delay of flame acceleration for a delayed detonation. Furthermore, the argumentation of § 2.4 concerning the transport and burning timescales is still true, so that equation (10) still holds on every scale above the Gibson length (which now, of course, decreases according to the increasing strength of turbulence). More complicated, scale-dependent feedback mechanisms would also alter the spectrum of turbulent velocities, giving rise to a fractal dimension of the flame surface different from $D \approx 7/3$.

A recent proposal by Kerstein (1996) gives strong support to the idea of active turbulent combustion. The author states that power-law growth of the turbulent burning velocity (as opposed to exponential growth expressed by eq. [16]) naturally occurs in the absence of a stabilizing mechanism, either by self-acceleration or through a statistical effect. However, the growth exponent is sensitive to the underlying model of flame dynamics and thus remains undetermined.

As there is no natural limit for this growth in the incompressible regime, the velocity of turbulent eddies on large scales would eventually exceed that of rising RT bubbles (eq. [11]). From there on, the properties of the flame brush would be independent of the RT instability. As the turbulent velocities become close to sonic, compressibility effects grow more important and may give rise to a delayed detonation (see § 3.2.4). It must be noted that this self-enhancement effect can only occur after the cellular structure has been disrupted above the Gibson scale by the turbulent cascade from larger scales. This, together with the increasing gas expansion as the star expands, may explain the delay in the acceleration of the turbulent burning front necessary to account for SN Ia nucleosynthesis. We emphasize again that the arguments given here are speculation and need to be confirmed experimentally or numerically. Three-dimensional simulations of burning in a preturbulized medium covering as many scales as reasonable are needed.

3.1.3. *Initial Conditions: Multipoint Ignition*

As pointed out by Garcia-Senz & Woosley (1995) and demonstrated by Niemeyer et al. (1996), the efficiency of a white dwarf deflagration is sensitive to the manner in which the runaway is initiated. Multiple-point ignition a few hundred kilometers out from the center gives more powerful explosions than one ignited at the stellar center. This is because burning bubbles born off-center are more buoyant at birth because of the higher gravity and can travel farther before the star begins to disrupt.

It is presently uncertain how far this trend can be continued. Obviously a white dwarf ignited simultaneously at a large number of points scattered uniformly throughout its mass would have no difficulty exploding, but that would be artificial. The condition of simultaneity requires synchronization of the burning in regions that, at the time they run away, are out of communication. The calculations of Garcia-Senz & Woosley (1995) indicate that it would take an extremely fine tuning of the temperature in order to get a convective bubble in the phase immediately preceding runaway to float more than ~ 200 km. Still, a large number of 10 km bubbles, say, could be crowded onto a sphere of this radius. If these floated a large distance after burning before acquiring sufficient velocity to drive lateral burning by the KH instability and turbulence, the effective burning rate could become quite large (picture a dandelion gone to seed as the location of burned ash at this point). The time-dependent competition between lateral and radial burning is thus important. Three-dimensional calculations to explore this possibility would be interesting.

3.2. *Detonation*

The simplest form of explosion, insofar as the hydrodynamics is concerned, would be detonation. This was the solution originally proposed by Arnett (1969), but numerous variations have been proposed since then that differ in where and when the transition from subsonic to supersonic burning occurs. In order to make this transition, it is necessary that some volume sufficiently large to maintain a detonation burn in a time short compared to that required for sound crossing. Before discussing specific models, we begin by deriving a grid of critical masses capable of igniting and sustaining a detonation. We concentrate on densities between 10^7 and 10^8 g cm^{-3} because this is the approximate range required for a transition to detonation that will provide ample intermediate-mass elements.

3.2.1. *Critical Masses for Detonation*

The general idea of a critical mass for detonation follows Blinnikov & Khokhlov (1986, 1987), Khokhlov (1991a), and Woosley (1990); see also He & Clavin (1994) for a recent analysis of critical conditions for detonations. A propagating detonation wave must exert sufficient overpressure to burn a region in a sound crossing time. If it does not, the shock will degenerate into a pressure wave and damp. The shock temperature for the self-consistent wave is given by the density and composition. This temperature gives a timescale for burning which, when multiplied by the sound speed, gives a rough estimate of the detonation wave thickness. Unless this distance is very small compared to the size of the region where the phase velocity of burning is supersonic, the detonation will damp.

We have determined empirically a series of critical masses using the one-dimensional hydrodynamics code KEPLER (Weaver et al. 1978), which has nuclear physics and an equation of state appropriate for the problem. The nuclear network employed contained 19 isotopes from hydrogen to ^{56}Ni. Radiation transport was turned off and only the quadratic artificial viscosity term employed. Spheres were constructed of 100 zones with the mass of each zone smoothly increasing outward (the first 30 zones had constant mass; the other 70 gradually increased logarithmically to a value 100 times larger than the central zone in zone 100). For the calculations at $\rho \leq 10^8$ g cm^{-3}, a linear (with respect to interior mass) temperature gradient was superimposed on the inner 28 zones with a central value of 3.2×10^9 K falling to 4×10^8 K in zone 28. The rest of the zones also had a temperature of 4×10^8 K. This temperature gradient was such as to give a well-resolved supersonic phase velocity for the burning in the inner zones for all spheres considered. The density was taken to be approximately constant in all zones and a boundary pressure applied to the sphere equal to that in the outer zones. For the $\rho = 2 \times 10^9$ g cm^{-3} case, the central temperature was assumed to be 2.8×10^9 K, declining smoothly over 55 zones to 7×10^8 K, where it remained constant for another 145 zones. A sample calculation is given in Figure 4.

Burning was then turned on and the subsequent evolution followed for about 4000 time steps in each case (20,000 in the case of 2×10^9 g cm^{-3}). Several dozen such spheres were modeled. A sampling of results is given in Table 1. In each case the critical mass is the lowest value for which detonation was achieved and maintained. The value given is the mass interior to zone 20, i.e., most of the material upon which the high burning temperature was imposed. In each case a calculation using 10 times less mass was also carried out and gave a failure. The length scale is thus resolved to about a factor of 2. Because the results depend so sensitively upon the composition, it was not worthwhile to attempt greater resolution.

For the case of 50% carbon and 50% oxygen our results agree well (within a factor of 10) with those of Arnett & Livne (1994b). However, we also explored the sensitivity to composition and found the mass fraction of carbon to be very important. At a density of 3×10^7 g cm^{-3}, for example, the critical mass is 5 orders of magnitude smaller for pure carbon than for a mixture of 50% C and O. The larger Q-value for the burning gives a higher burning temperature in the detonation, and the reactions are very temperature sensitive. On the other hand, the mass is 5 orders of magnitude *larger* if the fuel is 40% carbon and 60% silicon, and for 35% carbon and 65% silicon the critical mass is larger than the star. We calculated mixtures of silicon and carbon because, later, we shall consider the possibility of igniting a detonation in a region where ash and fuel have mixed. At these densities, carbon and oxygen burn to intermediate-mass elements, of which silicon is more representative than nickel. Apparently, for each density, there is a critical mass of contamination by ash that makes detonation impossible. But if the ash remains a small component, the required critical masses are quite small.

While the calculations were carried out for thoroughly mixed combinations, similar restrictions would apply to a region of thinly laminated, but unmixed, fuel and ash. The critical quantity is the overpressure produced in a region large compared to the mixing scale. Since the ashes have long since yielded their overpressure to sustaining the subsonic expansion of the star, only the contribution of the fuel

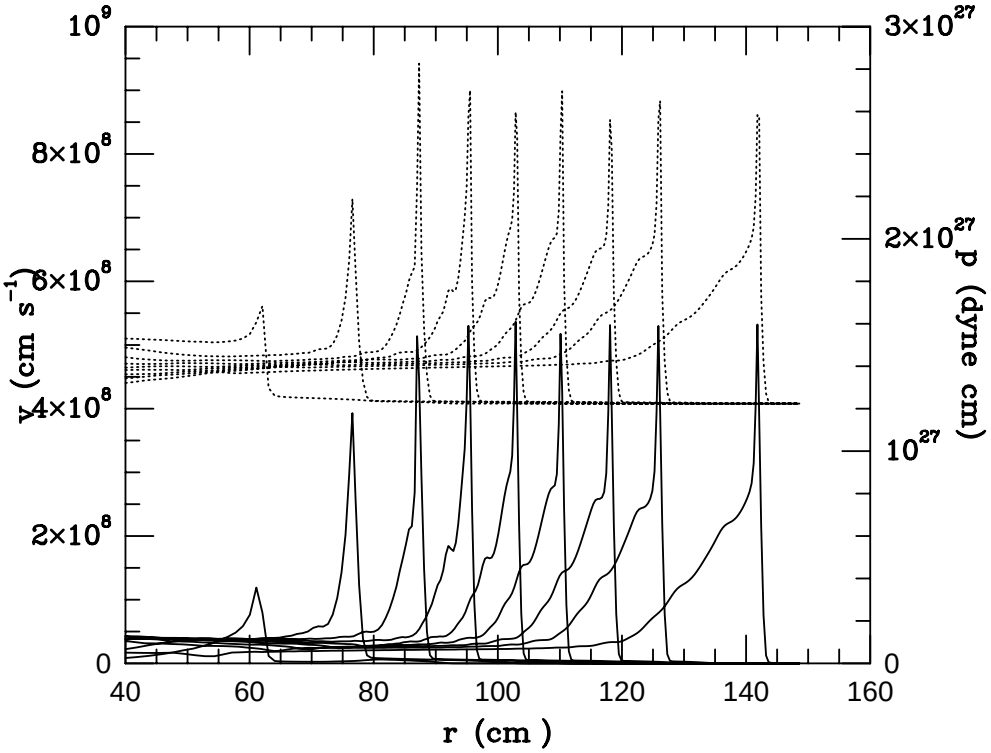

FIG. 4.—Microdetonation of a sphere of 50% carbon and 50% oxygen at 2×10^9 g cm^{-3}. The detonation was initiated by a temperature gradient that gave a supersonic phase velocity in the inner 70 cm ($10^{-18}\ M_\odot$). The temperature fell smoothly in the initial model to a constant background of 7×10^8 K at 87 cm ($2.7 \times 10^{-18}\ M_\odot$). The density jump in the steady state shock was 1.5. The times sampled in the figure are 0.66, 1.9, 2.6, 3.2, 3.8, 4.3, 4.8, 5.4, and 6.5×10^{-8} s. Velocity is the solid curve; pressure is the dashed curve.

is important. If the mass fraction of fuel in the macroscopic region is low, the critical mass is large.

These masses are for isolated hot spots surrounded by cold material. If the runaway occurs in an extended region that is itself close to burning on a sound crossing time, they could be smaller.

3.2.2. *Prompt Detonation*

We now discuss the possibilities for detonation in the approximate time order in which the detonation appears.

First, there is the possibility of a prompt detonation (Arnett 1969). Critical masses for prompt detonation have been calculated by Blinnikov & Khokhlov (1986, 1987) and are very small (see also Table 1 for $\rho = 2 \times 10^9$ g cm^{-3}), so there are an enormous number ($\sim 10^{18}$) of possibilities for detonation in the inner 100 km of the white dwarf that runs away. At issue, however, is the high degree of isothermality required to produce a supersonic phase velocity.

Woosley (1990) derives the condition that the phase velocity of nuclear burning be sonic in the presence of a temperature gradient dT/dr:

$$\left(\frac{dT}{dr}\right)_{\rm crit} = 0.3 T_9^{21.2} \rho_9^{3.05}\ {\rm K\ cm^{-1}}\ . \qquad (17)$$

Convection ceases to be efficient in transporting energy at about $T_9 = 0.7$, when the convective cycle time equals the nuclear burning time, and this is a convenient point at which to evaluate the isothermal condition. The above equation gives a critical gradient, $dT/dr \sim 0.001$ K cm^{-1}.

TABLE 1

CRITICAL MASSES

ρ	^{12}C	^{16}O	^{28}Si	^{56}Ni	Mass ($M_\odot$)	Radius	$T_{9\ \rm burn}$ (10 K)	$\tau^{\rm a}$ (s)
10^7	0.5	0.5	0	0	10^{-10}	2 km	3.5	4×10^{-4}
	0.5	0	0.5	0	10^{-8}	10 km	3.3	2×10^{-3}
3×10^7.....	1.0	0	0	0	10^{-19}	1 m	5.5	2×10^{-7}
	0.5	0.5	0	0	10^{-14}	50 m	5.2	1×10^{-5}
	0.5	0	0.5	0	10^{-10}	1 km	4.3	2×10^{-4}
	0.5	0	0	0.5	10^{-10}	1 km	4.1	2×10^{-4}
	0.4	0	0.6	0	10^{-5}	50 km	3.9	1×10^{-2}
	0.25	0.25	0.5	0	10^{-4}	100 km	4.0	2×10^{-1}
	0.35	0	0.65	0	$\gtrsim 10^{-1}$	...	...	...
10^8	1	0	0	0	10^{-20}	40 cm	6.5	1×10^{-7}
	0.5	0.5	0	0	10^{-18}	2 m	6.2	4×10^{-7}
	0.5	0	0.5	0	10^{-12}	150 m	5.5	3×10^{-5}
2×10^9.....	0.5	0.5	0	0	10^{-18}	70 cm	9.7	7×10^{-8}

[a] Sonic crossing time assuming a sound speed of 5000 km s^{-1} (10,000 at 2×10^9).

Conduction will tend to smooth out temperature fluctuations on small scales. For $\rho = 2 \times 10^9$ g cm^{-3} and $T_9 = 0.7$, the conductive opacity is about 10^{-5} cm^2 g^{-1} and the conductive length scale for 1 s is ~ 10 m. The timescale to increase nuclear energy generation at $T_9 = 0.7$ is ~ 10 s. Interestingly, the critical mass for detonation (Table 1) is also a few meters in radius, so perhaps an approximately isothermal region of this size is not unreasonable.

However, for detonation within a single critical mass of $10^{-18}\ M_\odot$ (Table 1), the temperature could only vary from $T_9 = 0.7$ by about one part in 10^{10} (if the conditions at $T_9 \approx 0.7$ evolved without outside influence to runaway)! For larger length scales, up to 10^7 cm, the restriction is less severe but still very constraining, about one part in 10^5. Further, this thermal condition must be maintained for an appreciable fraction of the nuclear timescale at $T_9 = 0.7$,

$$\tau_{\rm nuc} = 0.15 T_9^{-20.2} \rho_9^{-3.05} \approx 20 \text{ s} . \quad (18)$$

A prompt detonation becomes more likely if an only approximately isothermal region exists at higher temperature (eq. [17]). For example, consider the conditions after the runaway has progressed and the hottest temperature anywhere in the core is $T_9 = 1.2$. If this point is surrounded by, say, 10 km of material in which the temperature is between $T_9 = 1.2$ and $T_9 = 1.1$, a detonation will occur. Similarly, a point having $T_9 = 1.5$ must be surrounded by 10^4 cm of material between $T_9 = 1.4$ and 1.5, etc. However, the nuclear timescales at these points are 5×10^{-4} and 5×10^{-6} s, respectively, and there is no efficient energy transport mechanism that operates on such short times.

The actual thermal structure is not known with such precision. Small fluctuations will be amplified by the temperature sensitivity of the nuclear burning. Turbulence, energized by convection, has two effects. On the one hand, it acts to smooth out inhomogeneities. But, to the extent that the energy density in turbulence varies even slightly from place to place, different amounts of heat will be dissipated at the (very small) Kolmogorov scale. The convective velocity at $T_9 = 0.7$ is approximately 30 km s^{-1}. The energy density in this turbulence is about 10^{12}–10^{13} ergs g^{-1}; the heat capacity of the gas is $\sim 10^7$ ergs g^{-1} K^{-1}. The timescale for generating this energy is on the order of the convective turnover time 10–100 s. If 10% variations occurred in the dissipation rate in two regions, the temperature variation would be $\sim 10^5$ K. Although this does not prove that a prompt detonation is impossible, it suggests that it is much more difficult than the large number of critical masses implies.

The chief evidence against prompt detonation is not so much the physics of igniting the detonation as the fact that the models do not agree with observations. They produce too much ^{54}Fe with respect to ^{56}Fe and no intermediate-mass elements (e.g., Woosley 1990). The detonation wave may be unstable at high densities ($\rho \gtrsim 2 \times 10^7$ g cm^{-3}; Khokhlov 1993b), but the instabilities predicted act on scales of order 1 cm and less. This would have no effect on the nucleosynthesis, since even a laminar flame would burn through the residual fuel in less than an expansion time. If an instability were found that left behind regions of unburned material with the size ~ 100 km, these regions would not be completely burned by conduction in the explosion. The model would resemble the deflagration ignited at many points throughout its volume, discussed in the previous section. To our knowledge, no such instability has been proposed.

3.2.3. *Atmospheric Detonation*

The first models in which detonations were actually calculated rather than assumed (Nomoto et al. 1984; Woosley & Weaver 1986) occurred because a subsonic deflagration produced sufficiently strong pressure waves that their accumulation ahead of the flame led to compression adequate to ignite nuclear burning on a sonic time. This always occurred near the surface of the star in the steepening density gradient around 1.0–1.3 $M_\odot$. Such explosions made only a small quantity of intermediate-mass elements, but did produce very high velocity iron synthesized as ^{56}Ni near the surface. The high velocities may be necessary to explain some supernova observations, especially for SN 1991T (Yamaoka et al. 1992), but the small synthesis of Si–Ca remains a problem for the typical SN Ia. The reason so little silicon is made in these models is that the flame must move an appreciable fraction of the sound speed in order to steepen into a shock in the outer layers. Such rapid burning consumes the white dwarf before it has had time to expand and is still at high density.

To produce intermediate-mass elements, it is helpful if the supernova first burns relatively slowly and expands and then makes a transition to a detonation at a density $\sim 10^7$ g cm^{-1}. At such a low density, detonation proceeds not to iron but to silicon. This defines the "delayed detonation" model of Khokhlov (1991a, 1991b, 1991c) and Woosley & Weaver (1994).

3.2.4. *Delayed Detonation*

First we consider the model of Khokhlov, who attributes the transition to detonation to temperature fluctuations. These fluctuations arise from "nonuniform preheating of the gas" (or perhaps turbulence, though he emphasizes the former). Khokhlov points out that a spontaneous transition to detonation is frequently observed in terrestrial experiments (e.g., Lee & Moen 1980) involving turbulent flames. The underlying idea is similar to that discussed in § 3.2.2. A single small region, but one larger than the critical mass, burns faster than sound because of an anomalously high temperature and shallow temperature gradient. Once a detonation is initiated, even a small one, it propagates through the rest of the star.

However, such large localized temperature fluctuations are unlikely. As long as the flame retains a well-defined surface (i.e., operates in the laminar or "flamelet" regime; § 2.4), high fuel temperatures exist only in the thin interface separating fuel and ash. Burning in this interface is very subsonic (defining, in fact, the laminar speed) and the mass in a flame thickness is much less than a critical mass. Previously existing, isolated temperature fluctuations in the carbon fuel will tend to be damped and quenched by the expansion. By very careful tuning, one might arrange to have a disconnected region run away at a late time (burning would occur at a rate that, for a long time, precisely balanced adiabatic losses as in Garcia-Senz & Woosley 1995). Additional tuning could give this region such a shallow temperature gradient that it burned supersonically. Not only does this seem unlikely, but the runaway would be much more likely to occur at an earlier time and there would be nothing special to delay the burning until the density declined below 3×10^7 g cm^{-3}, as is necessary if intermediate-mass elements are to be produced.

Temperature fluctuations might also be built up by the collision of sound waves or blobs of matter moving in random directions in the unburned carbon, but the energy density of these collisions is small. Typical velocity shears are 100 km s^{-1}, implying an energy density of $\sim 10^{14}$ ergs g^{-1}. At a density of 3×10^7 g cm^{-3}, an internal energy addition of about 10^{17} ergs g^{-1} is required to raise the temperature above 2.0×10^9 K, where burning on a hydrodynamic timescale can occur. We conclude that a delayed detonation initiated by temperature fluctuations is unlikely.

A different sort of delayed detonation was discussed by Woosley & Weaver (1994) in lectures presented at Les Houches in 1990. This kind of model resembles more the atmospheric detonations of § 3.2.3, but there is an attempt to "sculpt" the flame speed so as to provoke a detonation in a star with initially slow burning. In outcome the model is the same as that of Khokhlov, but the detonation occurs because of an accumulation of overpressure in a macroscopic region surrounding a topologically complex flame surface. Geometry plays the key role, not temperature fluctuations or gradients, and it makes sense to cast the model in terms of the fractal dimension of the flame. Some representative conditions illustrate the idea. At 3×10^7 g cm^{-3}, the critical mass for detonation is around $10^{-14}\ M_\odot$ (50 m for 50% carbon; Table 1). The turbulent flame brush (§ 2.4) might be up to 200 km thick (i.e., it contains many critical masses; Niemeyer et al. 1996), the laminar speed of the flame about 0.5 km s^{-1}, the sound speed near 5000 km s^{-1}, and the smallest unstable wavelength about a centimeter. The 200 km thick region will then burn supersonically if the fractal dimension in that region exceeds 2.6.

There are several difficulties here. First, the fractal dimension associated with a turbulent flame is well pegged to 2.3–2.36, based upon both simple scaling relations (Kerstein 1988, 1991) and experiment (e.g., Mantzaras, Felton, & Bracco 1989; North & Santavicca 1990; Haslam & Ronney 1995). A value of 2.6 would require nonstandard assumptions (though Mandelbrot 1983 offers arguments that the fractal dimension of isoscalar surfaces in turbulence should be 2.5–2.66). It should be recognized, however, that $D = 7/3$ is a statistical average. There may be regions having larger dimension and others with smaller ones.

Why would this detonation occur preferentially at late times? At earlier times, the Gibson length is much larger and the structure of the flame brush correspondingly coarser. At 10^9 g cm^{-3}, for example, the laminar flame speed is about 50 km s^{-1}. A flame brush of 200 km (though none would exist yet at this early time) would have a sound crossing time of about 0.02 s, and the spacing between burning regions for supersonic effective burning would be 1 km. The Gibson length at these conditions is larger than 1 km; so too is the minimum unstable Rayleigh-Taylor wavelength (Timmes & Woosley 1992). It would be hard to prepare such a layered structure without burning all the fuel in the process. Detonation would be difficult.

A second condition required for a delayed detonation of this type is that the mass fraction of ash in the flame brush not be high. At 3×10^7 g cm^{-3}, Table 1 suggests that detonation would not occur if the ash comprised more than 35% of the mass of the flame brush.

We conclude that a delayed detonation of the kind proposed by Woosley & Weaver (1994) is possible, but its actual occurrence improbable. Whether the requisite fine structure can be set up is unknown.

3.2.5. *Detonation in the Distributed Regime*

Instead of mixing and wrinkling a thin flame sheet, turbulence, in the extreme, might mix heat from the ashes into cold unburned fuel. Rather than accumulate a critical surface area within a volume, the star might instead gradually build a critical temperature in a volume of fuel larger than in Table 1, as Khokhlov's model (1991a, 1991b, 1991c) requires. This sounds straightforward, but it can be difficult to arrange. Indeed, for densities above about 3×10^7 g cm^{-3}, without pulsation, it is impossible.

Above this density, the microphysics of the nuclear burning and electron conduction can be decoupled from all the instabilities we have discussed. Viewed on a sufficiently small scale (i.e., the conductive flame thickness), the flame is smooth and stable (Fig. 1). Since the thickness of the flame is smaller than any critical mass in Table 1, no detonation can occur.

However, as the density drops below about 3×10^7 g cm^{-3} (Fig. 2), nuclear burning proceeds at a slower rate and the flame becomes thicker. For a mixture of 50% carbon and 50% oxygen, Timmes & Woosley (1992) find a flame thickness of 0.5 cm at 5×10^7 g cm^{-3} and 4 cm for 1×10^7 g cm^{-3}. At the same time, the scale of the smallest turbulent eddies that can turn over without burning (the Gibson scale) grows progressively smaller. For a turbulent energy density of 10^{14} ergs g^{-1} at 10^6 cm (Niemeyer & Hillebrandt 1995b), the Gibson scale is 0.2 cm and 10^{-4} cm, respectively, at 5 and 1×10^7 g cm^{-3}. Somewhere between these two densities a transition to a different kind of burning must occur.

Under these conditions it no longer makes sense to speak of a flame propagated solely by electronic conduction. The burning is smeared out by turbulence; one enters the distributed regime of Figure 2. Heat can then be extracted from burning regions and transported to fuel. To make the transition to detonation a region of size larger than the critical mass (Table 1) must assume a temperature gradient shallower than that given by equation (17) with a peak temperature such that the nuclear burning time is much shorter than the stellar expansion time. We now illustrate, with specific conditions, how this might occur.

First, a portion of the flame brush moves into the distributed region. We take a density 3×10^7 g cm^{-3} as representative. The turbulent flame brush is, at this point, a fine-grained mixture of discrete phases—fuel and ash, fine-grained, but still separated. Now, in places, the burning begins to go out as turbulence penetrates the flame sheet, homogenizes the composition, and reduces the temperature to some low mean value where burning is very slow. Recall the physics of the laminar flame (Timmes & Woosley 1992). There is a critical temperature in the flame where conduction balances nuclear energy generation. The nuclear timescale at this temperature times the laminar flame speed equals its thickness. As the flame enters the distributed region, turbulent eddies with a size comparable to the flame thickness (~ 1 cm) become fast enough to carry away heated fuel before it can burn. One might say that turbulence, for the first time, "enters" the reaction region and disperses it to larger length scales, where, again, the burning time equals the (turbulent) transport time. For still lower densities and temperatures, and thus lower burning rates, the same level of turbulence is able to distribute the reaction zone on even larger scales.

This leads to regions where the burning is temporarily quenched. As the overall density declines, these regions grow in size and, if the star becomes unbound, eventually encompass all the flame brush. These regions of suppressed burning are still coupled by turbulence, however. An important timescale to keep in mind is the characteristic turbulent timescale for a critical mass (Table 1). We shall assume, and justify later, that the fraction of ash in the mixture is small. Taking carbon equals oxygen equals 50% by mass, the critical mass is $\sim 10^{-14}\ M_\odot$, and its size is 50 m. Its turbulent turnover time is then $\tau_{\rm crit} \sim 10^{-3}$ s (Fig. 1). It is important that this is very much less than the hydrodynamical time, $\tau_{\rm dyn} = 446/\rho^{1/2} \sim 0.1$ s, for the star to expand.

If the mixture of fuel and ash burns faster than $\tau_{\rm crit}$, mixing will be incomplete and no detonation is possible. This requires that the temperature of the mixture be less than $T_9 = 2.2$ (eq. [18]), cooler if one considers larger regions containing many critical masses. On the other hand, the mixture must be able to resume rapid burning during the hydrodynamic timescale, and that requires a temperature *larger* than $T_9 = 1.7$. For intermediate temperatures of the mixture, a detonation is possible. The temperature in the ashes of a typical deflagration when the density is 3×10^7 g cm^{-3} is $T_9 = 4$–5. The electronic heat capacity still dominates, so $C_v \propto C_v \propto T$. Therefore, mixing equal masses of fuel and ash gives a mixture with temperature $T_{\rm ash}/2^{1/2}$, with little dependence on the temperature in the cold fuel. If we want the mixture to have a temperature of $T_9 = 2$, for example, then each part of ash must be diluted with 5 parts of fuel if the unmixed ash has temperature $T_9 = 5$ and 3 parts fuel if it has temperature $T_9 = 4$. This justifies the use of the (ash-free) critical mass chosen above. The actual dilution factor must ultimately come from a numerical study that we are unable to do right now. If it is too large or too small, the model fails.

A delay follows during which the temperature rises and the mixture runs away. For a detonation to occur, a region larger than the critical mass must have a nearly isothermal temperature distribution (eq. [17]), about 20 K cm^{-1} if we continue to use our (very approximate) representative value of $T_9 = 2$. This means that once the mixture resumes burning, there can be no large region cooler than this peak value minus the temperature gradient times the size of the region (10^5 K for 50 m). The region can, of course, be larger than the critical mass and the condition on the temperature fluctuations less stringent, but larger regions will have longer turbulent timescales and it will be harder to mix them without the fuel already burning.

As in the case of prompt detonation (§ 3.2.2), one has many opportunities for an improbable event, so the outcome is uncertain. However, because of the higher characteristic temperature ($T_9 \approx 2$ rather than $T_9 \approx 0.7$), the isothermal condition is not nearly so stringent, and with as many as $\sim 10^{12}$ critical masses in the flame brush a detonation does not seem so unlikely. The congruence of the density where distributed burning can begin with that required for a detonation to make appreciable intermediate-mass elements is also particularly encouraging for this model—another key difference with the prompt detonation model.

3.2.6. *Pulsational Detonation*

If inadequate fuel burns to disrupt the white dwarf on the first pulse, contraction will cause rekindled combustion and one or more pulsations will ensue. The burning conditions after each pulse will differ appreciably from the one before. If the pulse does not go below $\sim 3 \times 10^7$ g cm^{-3}, the boundary between ash and fuel remains intact but the flame surface becomes dispersed throughout a greater fraction of the mass and more convoluted as well. If the pulse goes below $\sim 3 \times 10^7$ g cm^{-3}, turbulence will mix both the composition and the heat across the interface. During the recompression, a large region of shared energy (or of dispersed flame) will reignite, giving rise once more to the possibility of detonation, or at least very rapid combustion.

Models of this sort have been studied by Khokhlov (1991b), Khokhlov, Müller, & Höflich (1993), Höflich, Khokhlov, & Wheeler (1995) and, in two dimensions, by Arnett & Livne (1994a, 1994b) following early pioneering work on pulsational deflagration by Nomoto et al. (1976) and Ivanova et al. (1974). More recently Woosley (1996) has demonstrated, using mixing-length convection theory and a fractal flame in a one-dimensional model where pulsation was explicitly calculated, several possible outcomes including either detonation (the pulsational analog to § 3.2.4) or an accelerated deflagration. However, no previous calculation has properly considered the critical role of turbulence. Without turbulence, the surface topology is not made much more complex during the pulse, nor is heat appreciably shared between fuel and ash. The heated region is instead confined to a narrow layer on the surface of a conductive flame. This is the definition of the flame thickness and, for a monotonically expanding supernova, this thickness is, at all times, thinner than the critical mass for detonation. It is possible, in principle, for a very large amplitude pulsation to lead to such a thick conductive flame that, during recontraction, the heated region encompasses a critical mass, an approach taken, for example, by Arnett & Livne (1994b). But for the same conditions, turbulence would dominate the heat transport.

Observationally, the pulsational detonation model, or at least the single large pulse version, has a difficulty. If a large-amplitude pulse is necessary for the initiation of the detonation, one would expect *some* white dwarfs to explode weakly without pulsing at all. Why should all initial pulses fall just short of producing an explosion? These supernovae with their faint, broad light curves have, at the present time, no observational counterpart. Perhaps they await discovery. Or perhaps the explosion proceeds through a series of low-energy pulses, only the last of which is always adequate to provoke detonation. In the latter case, the density 3×10^7 g cm^{-3} is critical. Pulsations that do not go below this value would not lead to greatly accelerated burning because their flames would remain, on the small scale, laminar and dominated by conduction. The first pulsation to go below this density would experience appreciable mixing and heat sharing and greatly accelerated burning, perhaps detonation, on the next pulse. Burning on a hydrodynamic timescale would also be guaranteed, since burning would be responsible for halting the recompression.

What actually happens will not be known until realistic three-dimensional models (with realistic ignition conditions; § 3.1.3) have been calculated, both to show the failure of the first pulse and the degree of turbulent mixing during subsequent pulses.

4. CONCLUSIONS

Our first conclusion, perhaps not a very reassuring one to

the observers, is that there are a lot of models for how a white dwarf explodes, none of which can be definitely excluded. However, our analysis suggests that some models are more easily realized than others and provides calculations to clarify the situation.

The simplest model, plain carbon deflagration, is an area where progress can be and needs to be made. Currently one does not know whether or not the burning front is able to unbind the star without an intervening pulse, which would exclude the pulsational detonation model. If a radial front moves at the Sharp-Wheeler speed (eq. [13]), the star becomes unbound, but this assumes efficient combustion by turbulence within the RT mixing layer (§ 3.1.1). The radial velocity of the bubble front is set by the nonlinear Rayleigh-Taylor instability, which should advance at nearly the Sharp-Wheeler speed ($0.1 g_{\rm eff}\, t$). Behind the leading edge of the bubble front, burning is enhanced by turbulence generated by the Kelvin-Helmholtz instability in shear flows bounding the RT-unstable blobs. It is not clear that fuel consumption proceeds at the same speed as the bubble front moves into the fuel. In other words, a stationary turbulent flame brush may never be established during the explosion, in which case the burning speed remains smaller than the Sharp-Wheeler speed. High-resolution three-dimensional calculations should ultimately clarify the issue. If the two speeds are comparable, an explosion seems likely, if only a mild one. The success of the first pulse is also very dependent upon how the runaway is initiated in the star (§§ 3.1.1, 3.1.3).

If the simple deflagration succeeds, then, in order to agree with observations, it must have a higher speed than current multidimensional calculations suggest. We have discussed two possible ways of speeding it up: active turbulent combustion (§ 3.1.2) that increases the turbulence intensity by thermal expansion within the flame brush, and extreme multipoint ignition (§ 3.1.3). According to recent results for the scaling behavior of unconfined turbulent flames (Kerstein 1996), active turbulent combustion is a very promising field for future investigations, but its influence on the explosion mechanism remains speculative.

Delayed detonations without an intervening pulsation are also not excluded, but those in the current literature have problems (§ 3.2.4). The temperature fluctuations required to induce detonation by a "spontaneous burning" (Khokhlov 1991a, 1991b, 1991c) are unlikely, and the large fractal dimension and small minimum wavelength used by Woosley & Weaver (1994) are inconsistent with current views regarding turbulence. Indeed, in the current view, an effective burning speed, $u_{\rm tur}$, faster than the fastest turbulent motion, $v(L)$ (which occurs on the largest scale L), is impossible (§ 2.4). This form of delayed detonation model survives for the time being, because the Kolmogorov mean field description of turbulence may not fully describe our time-dependent situation. The relation $u_{\rm tur} \approx v(L)$ is an average. There may be appreciable fluctuations from this mean in isolated small regions larger than a critical mass (we are currently investigating this). Active turbulent combustion (§ 3.1.2) might enhance the fuel consumption rate sufficiently. Another possibility is a burning geometry that favored only radial growth early on but rapid nonradial combustion at late times.

A more likely possibility, which we are suggesting here in the astrophysical context for the first time, is a transition to detonation as the star expands, its density declines, and it enters the regime of distributed burning (Fig. 2; § 3.2.5). This kind of explosion has several appealing characteristics. First, the transition to detonation occurs as a deflagration is dying. This naturally leads to the desired preexpansion of the star and rapid burning at late times. In particular, abundant intermediate-mass elements can be synthesized at densities below the transition density, $\sim 10^7$ g cm^{-3}. If the detonation ignites, it will naturally give a very energetic explosion, currently a problem for the deflagrations. Most important, it does these things using credible, definite physics, which, though uncertain, can be tested by numerical modeling. At this point its greatest uncertainties are the actual dilution factor for fuel and ash (a value of one part ash to several parts fuel is optimal) and whether the necessary isothermal conditions can be set up in the mixed medium at $T_9 \approx 2$. *For these reasons, this is the model that we favor at the present time.* The observational consequences of this form of detonation should be the same as for other forms of (parameterized) delayed detonation models.

If the detonation fails to catch on the first try, and if simple deflagration fails, then pulsational detonation (§ 3.2.6) offers an appealing alternative, but not one without its own puzzles. The deflagration must fail after having burned an appreciable mass so that the dwarf experiences a large-amplitude oscillation. This requires some tuning so that the star does not become unbound and yet still expands enough to mix. Why do we see no supernovae that just barely exploded? Here again distributed burning may help. The detonation only lights once the pulsation has sufficient amplitude to go to 10^7 g cm^{-3} at which point efficient mixing occurs. The star could approach this limiting density by one or more pulsations.

Because fundamental physics does not yet preclude several qualitatively different outcomes from very similar starting points, it is possible that they all happen to some extent. Even within a single class of model there is room for considerable variation owing to different ignition conditions, variable ratios of carbon to oxygen (which set the underlying conductive speed as well as affect the critical detonation mass), and the uncertain transition to detonation. Such diversity may be necessary to understand such distinctively different Type Ia supernovae as SN 1991bg and SN 1991T.

This work has been supported by the National Science Foundation (NSF 91 15367 and 94 17161) and the NASA Theory Program (NAGW 2525 and NAGS-2843), and in Germany by a DAAD HSP II/AUFE fellowship (J. C. N.) and a Humboldt Award (S. E. W.). We thank Sergei Blinnikov for a careful reading of the manuscript and useful comments, and Wolfgang Hillebrandt for informative discussions. We are particularly indebted to Alan Kerstein of Sandia Laboratory for several illuminating discussions regarding turbulent chemical combustion.

REFERENCES

Arnett, W. D. 1969, Ap&SS, 5, 280
Arnett, W. D., & Livne, E. 1994a, ApJ, 427, 315
———. 1994b, ApJ, 427, 330
Blinnikov, S. I., & Khokhlov, A. 1986, Soviet Astron. Lett., 12, 131
———. 1987, Soviet Astron. Lett., 13, 364
Blinnikov, S. I., & Sasorov, P. V. 1996, Phys. Rev. E, 53, 4827

Bychkov, V. V., & Liberman, M. A. 1995, A&A, 302, 727
Chandrasekhar, S. 1961, Hydrodynamic and Hydromagnetic Stability (Oxford: Oxford Univ. Press)
Clavin, P. 1990, in Fluid Dynamical Aspects of Combustion Theory, ed. M. Onofri & A. Tesei (Harlow: Longman), 43
———. 1994, Annu. Rev. Fluid Mech., 26, 321
Darrieus, G. 1938, in La Technique Moderne (unpublished)
Davies, R. M., & Taylor, G. 1949, Proc. R. Soc. London, A, 200, 375
Garcia-Senz, D., & Woosley, S. E. 1995, ApJ, 454, 895
Glimm, J., & Li, X. L. 1988, Phys. Fluids, 31, 2077
Haslam, B. D., & Ronney, P. D. 1995, Phys. Fluids, 7, 1931
He, L. T., & Clavin, P. J. 1994, J. Fluid. Mech., 277, 227
Höflich, P., Khokhlov, A., & Wheeler, J. C. 1995, ApJ, 444, 831
Ivanova, L. N., Imshennik, V. S., & Chechetkin, V. M. 1974, Ap&SS, 31, 497
Kerstein, A. 1988, Combustion Sci. Technol., 50, 441
———. 1991, Phys. Rev. A, 44, 3633
———. 1996, Combustion Sci. Technol., in press
Khokhlov, A. M. 1991a, A&A, 246, 383
———. 1991b, A&A, 245, L25
———. 1991c, A&A, 245, 114
———. 1993a, ApJ, 419, L77
———. 1993b, ApJ, 419, 220
———. 1995, ApJ, 449, 695
Khokhlov, A. M., Müller, E., & Höflich, P. 1993, A&A, 270, 223
Landau, L. D. 1944, Acta Physicochim. URSS, 19, 77
Landau, L. D., & Lifshitz, E. M. 1991, Lehrbuch der theoretischen Physik, Vol. 6, Hydrodynamik (Berlin: Akademie-Verlag)
Layzer, D. 1955, ApJ, 122, 1
Lee, J. H. S., & Moen, I. O. 1980, Prog. Energy Combustion Sci., 6, 359
Mandelbrot, B. B. 1983, The Fractal Geometry of Nature (New York: Freeman), chaps. 10 and 30
Mantzaras, J., Felton, P. G., & Bracco, F. V. 1989, Combustion Flame, 77, 295
Markstein, G. H. 1951, J. Aeronaut. Sci., 18, 199
Niemeyer, J. C., & Hillebrandt, W. 1995a, ApJ, 452, 779
Niemeyer, J. C. 1995b, ApJ, 452, 769
———. 1996, in Thermonuclear Supernovae, ed. R. Canal & P. Ruiz-Lapuente (Dordrecht: Kluwer), in press
Niemeyer, J. C., Hillebrandt, W., & Woosley, S. E. 1996, ApJ, in press
Nomoto, K., Sugimoto, D., & Neo, S. 1976, Ap&SS, 39, 137
Nomoto, K., Thielemann, F.-K., & Yokoi, K. 1984, 1993, ApJ, 286, 644
North, G. L., & Santavicca, D. A. 1990, Combustion Sci. Technol., 72, 215
Peters, N. 1988, in Proc. 21st Int. Symp. Combustion (Pittsburgh: Combustion Inst.), 1232
Pope, S. B. 1987, Annu. Rev. Fluid Mech., 19, 237
Read, K. I. 1984, Physica D, 12, 45
Sharp, D. H. 1984, Physica D, 12, 3
Snider, D. M., & Andrews, M. J. 1994, Phys. Fluids, 6, 3324
Timmes, F. X., & Woosley, S. E. 1992, ApJ, 396, 649
Weaver, T. A., Zimmerman, G. B., & Woosley, S. E. 1978, ApJ, 225, 1021
Woosley, S. E. 1990, in Supernovae, ed. A. G. Petschek (Berlin: Springer), 182
———. 1996, in Thermonuclear Supernovae, ed. R. Canal & P. Ruiz-Lapuente (Dordrecht: Kluwer), in press
Woosley, S. E., Axelrod, T. S., & Weaver, T. A. 1984, in Stellar Nucleosynthesis, ed. C. Chiosi & A. Renzini (Dordrecht: Reidel), 263
Woosley, S. E., & Weaver, T. A. 1986, in IAU Symp. 89, Radiation Hydrodynamics in Stars and Compact Objects, ed. D. Mihalas & K.-H. A. Winkler (Berlin: Springer), 91
———. 1994, in Les Houches, Session LIV, Supernovae, ed. S. Bludman, R. Mochkovitch, & J. Zinn-Justin (Amsterdam: North-Holland), 63
Yamaoka, H., Nomoto, K., Shigeyama, T., & Thielemann, F.-K. 1992, ApJ, 393, L55
Young, D. L. 1984, Physica D, 12, 32
Zeldovich, Ya. B. 1966, J. Appl. Mech. Tech. Phys., 7, 68
Zeldovich, Ya. B., Barenblatt, G. I., Librovich, V. B., & Makhviladze, G. M. 1985, The Mathematical Theory of Combustion and Explosions (New York: Plenum)
Zeldovich, Ya. B., Istratov, A. G., Kidin, N. I., & Librovich, V. B. 1980, Combustion Sci. Technol., 24, 1